

Koopman-Based Learning of Infinitesimal Generators without Operator Logarithm

Yiming Meng, Ruikun Zhou, Melkior Ornik, and Jun Liu

Abstract—The Koopman operator has gained significant attention in recent years for its ability to verify evolutionary properties of continuous-time nonlinear systems by lifting state variables into an infinite-dimensional linear vector space. The challenge remains in providing estimations for transitional properties pertaining to the system’s vector fields based on discrete-time observations. To retrieve such infinitesimal system transition information, leveraging the structure of Koopman operator learning, current literature focuses on developing techniques free of time derivatives through the use of the Koopman operator logarithm. However, the soundness of these methods has so far been demonstrated only for maintaining effectiveness within a restrictive function space, together with knowledge of the operator spectrum properties. To better adapt to the practical applications in learning and control of unknown systems, we propose a logarithm-free technique for learning the infinitesimal generator without disrupting the Koopman operator learning framework. This approach claims compatibility with other system verification tools using the same set of training data. We provide numerical examples to demonstrate its effectiveness in applications of system identification and stability prediction.

Index Terms—Unknown nonlinear systems, Koopman operators, infinitesimal generator, system identification, verification.

I. INTRODUCTION

Verification of dynamical system properties and achieving autonomy are two important directions for the future of industrial intelligence, with applications in numerous fields, including mathematical finance, automated vehicles, power systems, and other physical sciences.

Witnessing the success of problem-solving within the data paradigm, there has been a surge of interest in revealing the governing equations of continuous-time dynamical systems from time-series data to better understand the underlying physical laws [1], [2]. Additional interests in safety-critical industries include data-driven stability and safety analysis, prediction, and control. Techniques such as Lyapunov and barrier certificates have proven effective [3]–[7]. It is worth

This research was supported by NASA under grant numbers 80NSSC21K1030 and 80NSSC22M0070, as well as by the Air Force Office of Scientific Research under grant number FA9550-23-1-0131.

Yiming Meng is with the Coordinated Science Laboratory, University of Illinois Urbana-Champaign, Urbana, IL 61801, USA. yymeng@illinois.edu.

Ruikun Zhou is with the Department of Applied Mathematics, University of Waterloo, Waterloo ON N2L 3G1, Canada ruikun.zhou@uwaterloo.ca.

Melkior Ornik is with the Department of Aerospace Engineering and the Coordinated Science Laboratory, University of Illinois Urbana-Champaign, Urbana, IL 61801, USA. mornik@illinois.edu.

Jun Liu is with the Department of Applied Mathematics, University of Waterloo, Waterloo ON N2L 3G1, Canada j.liu@uwaterloo.ca.

noting, however, that these practical concerns require information on the vector fields, the value functions that abstract system performance, and the corresponding Lie derivatives, all underpinned by an understanding of the infinitesimal generator [8]–[12]. Considering nonlinear effects, challenges therefore arise in the converse identification of infinitesimal system transitions based on discrete-time observations that represent cumulative trajectory behaviors.

For autonomous dynamical systems, direct methods such as Bayesian approaches [13] and the sparse identification of non-linear dynamics (SINDy) algorithm [14] have been developed to identify state dynamics with a known structure, relying on nonlinear parameter estimation [15], [16] and static linear regression techniques. However, these methods require that time derivatives of the state can be accurately estimated, an assumption that may not be robustly satisfied due to potential challenges such as low sampling rates, noisy measurements, and short observation periods. Furthermore, the data cannot be reused in the proposed structure for constructing other value functions (e.g., Lyapunov or barrier functions) for stability, reachability, and safety analysis. This limitation extends to verifying their Lie derivatives along the trajectories, which is crucial for demonstrating the evolving trends of the phase portraits.

Comparatively, the Koopman operator learning structure, achieved through linear least squares optimization over observable data of dictionary functions, does not require the estimation of time derivatives. It facilitates indirect learning of its infinitesimal generator, thus enabling a data-driven estimation of Lie derivatives with the same set of training data. This approach can potentially circumvent the need for high sampling rates and longer observation periods.

As observed in the current literature, this Koopman-based indirect learning of the infinitesimal generator heavily relies on the use of operator logarithms [17]–[20]. Heuristically, researchers tend to represent the Koopman operator \mathcal{K}_t by an exponential form of its infinitesimal generator \mathcal{L} as $\mathcal{K}_t = e^{t\mathcal{L}}$, leading to the converse representation $\mathcal{L} = \frac{1}{t} \log(\mathcal{K}_t)$ for any $t > 0$. However, problems arise given the following concerns: 1) representing Koopman operators in exponential form requires the boundedness of the generator \mathcal{L} ; 2) the operator logarithm as a single-valued mapping only within a specific sector of the spectrum; 3) for general systems that fall short of the aforementioned restrictions, it is unclear how the data-driven approximation of the logarithm of Koopman operators converges to the true generator.

As a complement to the work in [17], [19], recent studies [21], [22] have investigated the sufficient and necessary con-

ditions under which the Koopman-logarithm based generator learning method can guarantee learning accuracy. To provide the sampling rate, the theorem heavily relies on the concept of a “generator-bounded space”, which remains invariant under the Koopman operator, and where the generator is bounded when restricted to it. Though the results appear to be sound, the conditions are less likely to be verifiable for unknown systems.

To address the aforementioned issues, our goal in this paper is to propose a generator learning scheme that is robust to the choice of the dictionary of observable functions, without the need to know the spectrum properties. This scheme will be compatible with the current advances in [7] for Koopman-based construction of maximal Lyapunov functions. It is important to note that the method in [7] assumes full knowledge of the equilibrium point and acknowledges that verification of the constructed Lyapunov function depends on information about the actual system transitions, which may diminish its predictive value in stability analysis. Our approach aims to enhance Koopman-based learning approaches and align with the generator learning procedures, thereby achieving intelligent system identification and enabling automatic stability prediction.

Notation: We denote by \mathbb{R}^n the Euclidean space of dimension $n > 1$, and by \mathbb{R} the set of real numbers. For $x \in \mathbb{R}^n$ and $r \geq 0$, we denote the ball of radius r centered at x by $\mathcal{B}(x, r) = \{y \in \mathbb{R}^n : |y - x| \leq r\}$, where $|\cdot|$ is the Euclidean norm. For a closed set $A \subset \mathbb{R}^n$ and $x \in \mathbb{R}^n$, we denote the distance from x to A by $|x|_A = \inf_{y \in A} |x - y|$ and r -neighborhood of A by $\mathcal{B}(A, r) = \cup_{x \in A} \mathcal{B}(x, r) = \{x \in \mathbb{R}^n : |x|_A \leq r\}$. For a set $A \subseteq \mathbb{R}^n$, \bar{A} denotes its closure, $\text{int}(A)$ denotes its interior and ∂A denotes its boundary. For finite-dimensional matrices, we use the Frobenius norm $\|\cdot\|_F$ as the metric. Let $C(\Omega)$ be the set of continuous functions with domain Ω . We denote the set of i times continuously differentiable functions by $C^i(\Omega)$.

II. PRELIMINARIES

A. Dynamical Systems

Given a pre-compact state space $\mathcal{X} \subseteq \mathbb{R}^n$, we consider a continuous-time nonlinear dynamical system of the form

$$\dot{\mathbf{x}}(t) = f(\mathbf{x}(t)), \quad \mathbf{x}(0) = x \in \mathcal{X}, \quad t \in [0, \infty), \quad (1)$$

where x denotes the initial condition, and the vector field $f : \mathcal{X} \rightarrow \mathcal{X}$ is assumed to be locally Lipschitz continuous.

On the maximal interval of existence $\mathcal{I} \subseteq [0, \infty)$, the forward flow map (solution map) $\phi : \mathcal{I} \times \mathcal{X} \rightarrow \mathcal{X}$ should satisfy 1) $\partial_t(\phi(t, x)) = f(\phi(t, x))$, 2) $\phi(0, x) = x$, and 3) $\phi(s, \phi(t, x)) = \phi(t + s, x)$ for all $t, s \in \mathcal{I}$.

Throughout the paper, we will assume that the maximal interval of existence of the (unique) flow map to the initial value problem (1) is $\mathcal{I} = [0, \infty)$.

Remark 2.1: The above assumption is equivalent to assuming that the system exhibits forward invariance w.r.t. the set \mathcal{X} . However, this is usually not the case for general nonlinear systems. In this paper, if the system dynamics

violate the above assumption, we can adopt the approach outlined in [7, Section III.B] to recast the dynamics within the set $\bar{\mathcal{X}}$. In other words, we constrain the vector field f such that $f(x) = 0$ for any $x \in \partial\mathcal{X}$, while f remains unchanged within the open domain \mathcal{X} . This modification ensures that the system data is always collectible within $\bar{\mathcal{X}}$. \diamond

B. Koopman Operators and the Infinitesimal Generator

Let us now consider a complete normed function space $(\mathcal{F}, \|\cdot\|_{\mathcal{F}})$ of the real-valued observable functions $h : \mathcal{X} \rightarrow \mathbb{R}$. For any bounded linear operator $B : \mathcal{F} \rightarrow \mathcal{F}$, we define the operator (uniform) norm as $\|B\| := \sup_{\|h\|_{\mathcal{F}}=1} \|Bh\|_{\mathcal{F}}$. We clarify that in the context of operator learning, the term “observable functions,” or simply “observables,” commonly refers to “test functions” for operators, rather than to the concept of “observability” in control systems.

Definition 2.2: A one parameter family $\{\mathcal{S}_t\}_{t \geq 0}$ of bounded linear operators from \mathcal{F} into \mathcal{F} is a semigroup if

- 1) $\mathcal{S}_0 = \text{I}$ (I is the identity operator).
- 2) $\mathcal{S}_t \circ \mathcal{S}_s = \mathcal{S}_{t+s}$ for every $t, s \geq 0$.

In addition, a semigroup $\{\mathcal{S}_t\}_{t \geq 0}$ is a C_0 semigroup if $\lim_{t \downarrow 0} \mathcal{S}_t h = h$ for all $h \in \mathcal{F}$, and moreover a C_0 semigroup of contractions if $\|\mathcal{S}_t\| \leq 1$ for $t \geq 0$.

The (infinitesimal) generator A of $\{\mathcal{S}_t\}_{t \geq 0}$ is defined by

$$Ah(x) := \lim_{t \rightarrow 0} \frac{\mathcal{S}_t h(x) - h(x)}{t}, \quad (2)$$

where the observable functions are within the domain of A , defined as $\text{dom}(A) = \{h \in \mathcal{F} : \lim_{t \rightarrow 0} \frac{\mathcal{S}_t h - h}{t} \text{ exists}\}$. \diamond

It is a well-known result that $\text{dom}(A) = \mathcal{F}$.

The evolution of observables of system (1) restricted to \mathcal{F} is governed by the family of Koopman operators, as defined below. Koopman operators also form a linear C_0 semigroup, allowing us to study nonlinear dynamics through the infinite-dimensional lifted space of observable functions, which exhibit linear dynamics.

Definition 2.3: The Koopman operator family $\{\mathcal{K}_t\}_{t \geq 0}$ of system (1) is a collection of maps $\mathcal{K}_t : \mathcal{F} \rightarrow \mathcal{F}$ defined by

$$\mathcal{K}_t h = h \circ \phi(t, \cdot), \quad h \in \mathcal{F} \quad (3)$$

for each $t \geq 0$, where \circ is the composition operator. The (infinitesimal) generator \mathcal{L} of $\{\mathcal{K}_t\}_{t \geq 0}$ is defined accordingly as in (2). \diamond

Given that the observable functions are continuously differentiable, the generator of Koopman operators is such that $\mathcal{L}h(x) = \nabla h(x) \cdot f(x)$ for all $h \in C^1(\mathcal{X})$.

There is literature that, although focused on stochastic differential equations [23], [24], relies on the definition (2) to learn the generator. Despite the theoretical soundness, sampling trajectory information within an arbitrarily small time horizon is not practical.

C. Representation of Semigroups

In this subsection, we introduce basic operator topologies and explore how a semigroup $\{\mathcal{S}_t\}_{t \geq 0}$ can be represented through its generator A .

Definition 2.4 (Operator Topologies): Let $(\mathcal{F}, \|\cdot\|_{\mathcal{F}})$. Let $B : \mathcal{F} \rightarrow \mathcal{F}$ and $B_n : \mathcal{F} \rightarrow \mathcal{F}$, for each $n \in \mathbb{N}$, be linear operators.

- 1) The $\{B_n\}_{n \in \mathbb{N}}$ is said to converge to B *uniformly*, denoted by $B_n \rightarrow B$, if $\lim_{n \rightarrow \infty} \|B_n - B\| = 0$. We also write $B = \lim_{n \rightarrow \infty} B_n$.
- 2) The $\{B_n\}_{n \in \mathbb{N}}$ is said to converge to B *strongly*, denoted by $B_n \rightharpoonup B$, if $\lim_{n \rightarrow \infty} \|B_n h - B h\|_{\mathcal{F}} = 0$ for each $h \in \mathcal{F}$. We also write $B = \text{s-}\lim_{n \rightarrow \infty} B_n$. \diamond

Remark 2.5: In analogy to the pointwise convergence of functions, the strong topology is the coarsest topology such that $B \mapsto B h$ is continuous in B for each fixed $h \in \mathcal{F}$. \diamond

If A is a bounded linear operator that generates $\{\mathcal{S}_t\}$, then $\mathcal{S}_t = e^{tA}$ for each t in the uniform topology. Otherwise, [25, Chap. I, Theorem 5.5] still provides an interpretation for the sense in which \mathcal{S}_t “equals” e^{tA} .

We revisit some facts to show the above concepts of equivalence, particularly in the context where A is unbounded.

Definition 2.6 (Resolvents): Let A be a linear, not necessarily bounded, operator. Then the resolvent set is defined as

$$\rho(A) := \{\lambda \in \mathbb{C} : \lambda I - A \text{ is invertible}\}. \quad (4)$$

For any $\lambda \in \rho(A)$, the resolvent operator is defined as

$$R(\lambda; A) := (\lambda I - A)^{-1}, \quad (5)$$

which is a bounded linear operator [25, Chap. I, Theorem 4.3]. \diamond

We further define the *Yosida approximation* of A as

$$A_\lambda := \lambda A R(\lambda; A) = \lambda^2 R(\lambda; A) - \lambda I. \quad (6)$$

Note that $\{A_\lambda\}_{\lambda \in \rho(A)}$ is a family of bounded linear operators, and e^{tA_λ} is well-defined for each $\lambda \in \rho(A)$.

Theorem 2.7: [25, Chap. I, Theorem 5.5] Suppose $\{\mathcal{S}_t\}_{t \geq 0}$ is a C_0 semigroup on \mathcal{F} and A is the generator. Then, $\mathcal{S}_t = \text{s-}\lim_{\lambda \rightarrow \infty} e^{tA_\lambda}$ for all $t \geq 0$.

III. THE CHARACTERIZATION OF THE INFINITESIMAL GENERATORS

For system (1), we are able to represent \mathcal{K}_t as $e^{t\mathcal{L}}$ for bounded \mathcal{L} , or, by Theorem 2.7, as the strong limit of $e^{t\mathcal{L}_\lambda}$, where \mathcal{L}_λ is the Yosida approximation of the unbounded \mathcal{L} .

For the converse representation of \mathcal{L} based on $\{\mathcal{K}_t\}_{t \geq 0}$, it is intuitive to take the operator logarithm such that $\mathcal{L} = \frac{1}{t} \log \mathcal{K}_t$. When \mathcal{L} is bounded, the spectrum’s sector should be confined to make the logarithm a single-valued mapping [21], [22]. However, for an unbounded \mathcal{L} , there is no direct connection. In this subsection, we review how \mathcal{L} can be properly approximated based on $\{\mathcal{K}_t\}_{t \geq 0}$.

Due to the (local) Lipschitz continuity of f in (1), and considering that observable functions are usually continuous, we will focus on $\mathcal{K}_t : C(\mathcal{X}) \rightarrow C(\mathcal{X})$ for the rest of the paper. Then, $\mathcal{L} : C^1(\mathcal{X}) \rightarrow C(\mathcal{X})$. Let $C(\mathcal{X})$ be endowed with the uniform norm $|\cdot|_{\infty} := \sup_{x \in \mathcal{X}} |\cdot|$. Defining

$$|\cdot|_{\mathcal{L}} := |\cdot|_{\infty} + |\mathcal{L} \cdot|_{\infty}, \quad (7)$$

it can be shown that $|\cdot|_{\mathcal{L}}$ is equivalent to the C_1 -uniform norm. Consequently $(\text{dom}(\mathcal{L}), |\cdot|_{\mathcal{L}})$ is a Banach space.

A. Asymptotic Approximations of Generators

First, we examine the base case where $\{\mathcal{K}_t\}_{t \geq 0}$ is a contraction semigroup. In this situation, by the famous Hille-Yosida theorem [25, Theorem 3.1, Chapter I], the resolvent set is such that $\rho(\mathcal{L}) \supseteq \mathbb{R}^+$, and for each $\lambda \in \rho(\mathcal{L})$, we have $\|R(\lambda; \mathcal{L})\| \leq 1/\text{Re}(\lambda)$. Consequently, by [25, Lemma 1.3.3], $\{\mathcal{L}_\lambda\}_{\lambda > 0}$ converges in a strong sense to \mathcal{L} (w.r.t. $|\cdot|_{\mathcal{L}}$), i.e.,

$$\text{s-}\lim_{\lambda \rightarrow \infty} \mathcal{L}_\lambda = \text{s-}\lim_{\lambda \rightarrow \infty} \lambda^2 R(\lambda; A) - \lambda I = \mathcal{L}. \quad (8)$$

Moreover, the convergence rate is $\lambda^{-1} |\mathcal{L} h|_{\mathcal{L}}$ for all $h \in C^2(\mathcal{X})$, i.e. $|\mathcal{L}_\lambda h - \mathcal{L} h|_{\infty} \leq \lambda^{-1} |\mathcal{L} h|_{\mathcal{L}}$.

Remark 3.1: Due to the contraction restriction of $\{\mathcal{K}_t\}_{t \geq 0}$, the system (1) is necessarily *dissipative* [25, Chapt. I, Theorem 4.3]. As characterized in [26], it is equivalent to verifying the existence of a value (storage) function $V : \mathcal{X} \rightarrow \mathbb{R}^+$ and a (supply) function $\eta : \mathcal{X} \rightarrow \mathbb{R}$ satisfying $\int_s^t |\mathcal{K}_\tau \eta(x)| d\tau < \infty$, for all $s \leq t$ and all $x \in \mathcal{X}$, such that $\mathcal{K}_{t-s} V(x) - V(x) \leq \int_s^t \mathcal{K}_\tau \eta(x) d\tau$. In other words, the energy storage rate of the system cannot exceed η . This assumption is somewhat restrictive when considering unknown systems. \diamond

To accommodate more general cases, we propose the following extension of the Yosida approximation on \mathbb{R}^+ . To achieve this, we first present the following facts.

Proposition 3.2: For system (1), there exist constants $\omega \geq 0$ and $M \geq 1$ such that $\|\mathcal{K}_t\| \leq M e^{\omega t}$ for all $t \geq 0$. In addition, for any $\lambda \in \mathbb{C}$, the family $\{\mathcal{K}_{t,\lambda}\}_{t \geq 0}$, where

$$\mathcal{K}_{t,\lambda} := e^{\lambda t} \mathcal{K}_t \quad (9)$$

is a C_0 semigroup with generator $\mathcal{L} + \lambda I : \text{dom}(\mathcal{L}) \rightarrow C(\mathcal{X})$.

Proof: The first part follows directly by [25, Theorem 1.2.2]. The semigroup property of $\{\mathcal{K}_{t,\lambda}\}_{t \geq 0}$ follows easily by the definition. To verify its generator, we have $\frac{\mathcal{K}_{t,\lambda} h - h}{t} = \frac{e^{\lambda t} \mathcal{K}_t h - e^{\lambda t} h}{t} + \frac{e^{\lambda t} h - h}{t}$. For all $h \in \text{dom}(\mathcal{L})$, the limit exists as $t \downarrow 0$ for each r.h.s. term. It then follows that $\lim_{t \downarrow 0} \frac{\mathcal{K}_{t,\lambda} h - h}{t} = \mathcal{L} + \lambda I$. \blacksquare

Although it has been demonstrated in extensive literature that $\text{s-}\lim_{\lambda \rightarrow \infty} \mathcal{L}_\lambda = \mathcal{L}$ for $\{\mathcal{L}_\lambda\}_{\lambda > \omega}$, to better understand how data-driven approaches can be integrated into the approximation scheme, we prove the following theorem and demonstrate an explicit convergence rate.

Theorem 3.3: For system (1), let $\{\mathcal{L}_\lambda\}_{\lambda > \tilde{\omega}}$, where $\tilde{\omega} \geq \omega > 0$. Then, $\text{s-}\lim_{\lambda \rightarrow \infty} \mathcal{L}_\lambda = \mathcal{L}$. Moreover, for any $h \in C^2(\mathcal{X})$, there exists an $\tilde{M} > 0$ such that

$$|\mathcal{L}_\lambda h - \mathcal{L} h|_{\infty} \leq \tilde{M} (\lambda - \tilde{\omega})^{-1} (|h|_{\mathcal{L}} + |\mathcal{L} h|_{\mathcal{L}}).$$

Proof: For any $\tilde{\omega} \geq \omega$, we consider $\{\mathcal{K}_{t,-\tilde{\omega}}\}_{t \geq 0}$, where $\mathcal{K}_{t,-\tilde{\omega}}$ is defined as (9). It is clear that $\|\mathcal{K}_{t,-\tilde{\omega}}\| \leq M$ for all $t \geq 0$. By Proposition 3.2, $\{\mathcal{K}_{t,-\tilde{\omega}}\}_{t \geq 0}$ also admits the generator $\mathcal{L} - \tilde{\omega} I$. On $C^1(\mathcal{X})$, for any $\lambda > \tilde{\omega}$, we have

$$\begin{aligned} \mathcal{L} - \mathcal{L}_\lambda &= \mathcal{L} - \tilde{\omega} I + \tilde{\omega} I - \mathcal{L}_\lambda \\ &= (\mathcal{L} - \tilde{\omega} I - (\mathcal{L} - \tilde{\omega} I)_{\lambda - \tilde{\omega}}) \\ &\quad + ((\mathcal{L} - \tilde{\omega} I)_{\lambda - \tilde{\omega}} + \tilde{\omega} I - \mathcal{L}_\lambda) \\ &=: O_1 + O_2. \end{aligned} \quad (10)$$

It suffices to show the bound for each of the two terms on the r.h.s. of (10).

To show the bound for O_1 , we consider an alternative norm for $h \in C^1(\mathcal{X})$, defined as $\|h\|_\infty = \sup_{t \geq 0} |\mathcal{K}_{t, -\tilde{\omega}} h|_\infty$. It can be verified that $|h|_\infty \leq \|h\|_\infty \leq M|h|_\infty$. For $|h|_\mathcal{L}$, we define the alternative norm $\|h\|_\mathcal{L} = \|h\|_\infty + \|\mathcal{L}h\|_\infty$. In addition, $\|\mathcal{K}_{t, -\tilde{\omega}} h\|_\infty = \sup_{s \geq 0} |\mathcal{K}_{s, -\tilde{\omega}} \mathcal{K}_{t, -\tilde{\omega}} h|_\infty \leq \sup_{s \geq 0} |\mathcal{K}_{s, -\tilde{\omega}} h|_\infty = \|h\|_\infty$, which demonstrate the contraction property w.r.t. $\|\cdot\|_\infty$. Then, for any $h \in C^2(\mathcal{X})$, $O_1 h = -(\mathcal{L} - \tilde{\omega} \mathbf{I})R(\lambda - \tilde{\omega}; \mathcal{L} - \tilde{\omega} \mathbf{I})(\mathcal{L} - \tilde{\omega} \mathbf{I})h$ and

$$\begin{aligned} |O_1 h|_\infty &\leq \|O_1 h\|_\infty \leq (\lambda - \tilde{\omega})^{-1} \|(\mathcal{L} - \tilde{\omega} \mathbf{I})h\|_\mathcal{L} \\ &\leq M(\lambda - \tilde{\omega})^{-1} \|(\mathcal{L} - \tilde{\omega} \mathbf{I})h\|_\mathcal{L} \\ &\leq M(\lambda - \tilde{\omega})^{-1} (\|\mathcal{L}h\|_\mathcal{L} + \tilde{\omega}|h|_\mathcal{L}), \end{aligned}$$

where the second inequality can be proved in the same way as in [25, Chap. I, Lemma 3.2]. Since $C^2(\mathcal{X})$ is dense in $C^1(\mathcal{X})$, and the operator O_1 is uniformly bounded [25, Theorem 1.3.1] and hence continuous on $C^1(\mathcal{X})$, we have

$$\mathcal{L} - \tilde{\omega} \mathbf{I} = \text{s-lim}_{\lambda \rightarrow \infty} (\mathcal{L} - \tilde{\omega} \mathbf{I})_{\lambda - \tilde{\omega}} \quad (11)$$

on $(C^1(\mathcal{X}), \|\cdot\|_\mathcal{L})$. Due to the norm equivalence $\|\cdot\|_\mathcal{L} \approx |\cdot|_\mathcal{L}$, the strong convergence (11) also holds on $(C^1(\mathcal{X}), |\cdot|_\mathcal{L})$.

We now work on the bound for O_2 . One can show by a direct calculation that, for any $h \in C^1(\mathcal{X})$,

$$\begin{aligned} |O_2 h|_\infty &= |2\tilde{\omega}h - \tilde{\omega}(2\lambda - \tilde{\omega})R(\lambda; \mathcal{L})h|_\infty \\ &= |\tilde{\omega}(\tilde{\omega}R(\lambda; \mathcal{L}) - 2\mathcal{L}R(\lambda; \mathcal{L}))h|_\infty \\ &\leq M(\lambda - \tilde{\omega})^{-1} (\tilde{\omega}^2|h|_\infty + 2\tilde{\omega}\|\mathcal{L}h\|_\infty) \\ &\leq M_0(\lambda - \tilde{\omega})^{-1} |h|_\mathcal{L}, \end{aligned} \quad (12)$$

where $M_0 = M \cdot \max\{\tilde{\omega}^2, 2\tilde{\omega}\}$.

The conclusion follows by combining both parts and considering $\lambda \rightarrow \infty$. ■

Remark 3.4: In the proof of Theorem 3.3, we have implicitly demonstrated the effects of M and ω in the semigroup estimation $\|\mathcal{K}_t\| \leq M e^{\omega t}$. Intuitively, M represents the uniform scaling of the magnitude of the Koopman operator, while ω indicates the dominant exponential growth or decay rate of the flow on $C(\mathcal{X})$.

Working within the semigroup topology, one can always convert a C_0 semigroup into a contraction semigroup and approximate the generator using this connection, i.e., $(\mathcal{L} - \tilde{\omega} \mathbf{I})_{\lambda - \tilde{\omega}} + \tilde{\omega} \mathbf{I}$. However, this is not necessary given that, for arbitrarily large λ , \mathcal{L}_λ is arbitrarily close to $(\mathcal{L} - \tilde{\omega} \mathbf{I})_{\lambda - \tilde{\omega}} + \tilde{\omega} \mathbf{I}$ in a strong sense. The convergence rate remains similar. ◊

B. Representation of Resolvent Operators

Motivated by representing \mathcal{L} by $\{\mathcal{K}_t\}_{t \geq 0}$ and the Yosida approximation for \mathcal{L} on $\{\lambda > \omega\}$, we establish a connection between $R(\lambda; \mathcal{L})$ and $\{\mathcal{K}_t\}_{t \geq 0}$.

Proposition 3.5: Let $R(\lambda)$ on $C(\mathcal{X})$ be defined by

$$R(\lambda)h := \int_0^\infty e^{-\lambda t} (\mathcal{K}_t h) dt. \quad (13)$$

Then, for all $\lambda > \omega$,

- 1) $R(\lambda)(\lambda \mathbf{I} - \mathcal{L})h = h$ for all $h \in C^1(\mathcal{X})$;
- 2) $(\lambda \mathbf{I} - \mathcal{L})R(\lambda)h = h$ for all $h \in C(\mathcal{X})$.

The proof follows the standard procedures of calculus and dynamic programming, and is completed in Appendix I.

Remark 3.6: Even though $R(\lambda)$ is well defined on $C(\mathcal{X})$, the commutative property between $R(\lambda)$ and $\lambda \mathbf{I} - \mathcal{L}$ only holds on $C^1(\mathcal{X})$. This domain aligns with the valid domain where $\mathcal{L} = \text{s-lim}_{\lambda \rightarrow \infty} \mathcal{L}_\lambda$. ◊

To use the approximation in Section III-A, we can replace $R(\lambda; \mathcal{L})$ with $R(\lambda)$. We can immediately conclude the following representation.

Corollary 3.7: For each $\lambda > \omega$,

$$\mathcal{L}_\lambda = \lambda^2 \int_0^\infty e^{-\lambda t} \mathcal{K}_t dt - \lambda \mathbf{I} \quad (14)$$

and $\mathcal{L}_\lambda \rightarrow \mathcal{L}$ on $C^1(\mathcal{X})$.

IV. KOOPMAN-BASED FINITE-DIMENSIONAL APPROXIMATION OF GENERATORS

To employ (14), the current form of $\int_0^\infty e^{-\lambda t} (\mathcal{K}_t) dt$ is not advantageous. In this section, we derive an approximation approach based on a finite-dimensional observable data.

A. Finite Time-Horizon Approximation

Observing the form of (14), we first define the following truncation integral operator.

Definition 4.1: For any $h \in C(\mathcal{X})$ and $\tau \geq 0$, we define $\mathcal{T}_\tau : C(\mathcal{X}) \rightarrow C(\mathcal{X})$ as

$$\mathcal{T}_\tau h(x) := \int_0^\tau e^{-\lambda s} \mathcal{K}_s h(x) ds. \quad (15)$$

We aim to demonstrate that for any arbitrarily large $\lambda \in \mathbb{R}$, the aforementioned truncation of the integral will not significantly ‘‘hurt’’ the accuracy of the approximation (14).

Theorem 4.2: Let $\tau \geq 0$ and $\lambda > \omega$ be fixed. Then, $\|\lambda^2 \mathcal{T}_\tau - \lambda \mathbf{I} - \mathcal{L}_\lambda\| \leq \frac{M\lambda^2}{\lambda - \omega} e^{-\lambda \tau}$ on $C^1(\mathcal{X})$.

Proof: Note that, for any $\lambda > \omega$,

$$\begin{aligned} \|R(\lambda)\| &\leq \int_0^\infty e^{-\lambda t} \|\mathcal{K}_t\| dt \\ &\leq \int_0^\infty M e^{-\lambda t} e^{\omega t} dt = \frac{M}{\lambda - \omega}. \end{aligned} \quad (16)$$

Therefore, for any $h \in C(\mathcal{X})$,

$$\begin{aligned} |\mathcal{T}_\tau h - R(\lambda; \mathcal{L})h|_\infty &= \sup_{x \in \mathcal{X}} |e^{-\lambda \tau} R(\lambda)h(\phi(\tau, x))| \\ &\leq e^{-\lambda \tau} \|R(\lambda)\| \|h\|_\infty \leq e^{-\lambda \tau} \frac{M}{\lambda - \omega} |h|_\infty \end{aligned} \quad (17)$$

and $\sup_{|h|_\infty=1} |\lambda^2 \mathcal{T}_\tau h - \lambda h - \mathcal{L}_\lambda h|_\infty \leq \frac{M\lambda^2}{\lambda - \omega} e^{-\lambda \tau}$, which completes the proof. ■

We notice that $\lim_{\lambda \rightarrow \infty} \frac{\lambda^2}{\lambda - \omega} e^{-\lambda \tau} \leq \lim_{\lambda \rightarrow \infty} \frac{2}{\tau(\lambda - \omega)e^{\lambda \tau}}$ for any fixed τ , which demonstrates an exponential decaying rate in the uniform sense. Recalling the convergence rate of $\mathcal{L}_\lambda \rightarrow \mathcal{L}$ in Theorem 3.3, we note that the convergence in Theorem 4.2 does not dominate for any fixed $\tau > 0$. This allows us to use

$$\tilde{\mathcal{L}}_\lambda := \lambda^2 \mathcal{T}_\tau - \lambda \mathbf{I} \quad (18)$$

to approximate \mathcal{L} within a small time-horizon. We use the following example to illustrate this approximation.

Example 4.3: Consider the simple dynamical system $\dot{\mathbf{x}}(t) = \mathbf{x}(t)$ and the observable function $V(x) = x^n$ for any $n \geq 1$. Then, analytically, $\phi(\tau, x) = xe^\tau$ and $\mathcal{L}V(x) = nx^n$. We test the validity of using Eq. (18). Note that, for sufficiently large λ , we have $\lambda^2 \int_0^\tau e^{-\lambda s} (\mathcal{K}_s V(x)) ds = \lambda^2 \int_0^\tau e^{-\lambda s} x^{sn} ds = \frac{\lambda^2 x^n}{\lambda - n} (1 - e^{-(\lambda - n)\tau}) \approx \frac{\lambda^2 x^n}{\lambda - n}$, and $\lambda^2 \mathcal{T}_\tau V(x) - \lambda V(x) \approx \frac{\lambda^2 x^n}{\lambda - n} - \lambda x^n = \frac{n\lambda}{\lambda - n} x^n \approx nx^n = \mathcal{L}V(x)$. With high-accuracy evaluation of the integral, we can achieve a reasonably good approximation. \diamond

B. Finite-Rank Approximation

Based on (18), it suffices to learn the operator \mathcal{T}_τ for any fixed $\tau > 0$ and to predict the image of the operator when acting on some $C(\mathcal{X})$ function. In favor of a machine learning approach based on a dictionary of a finite number of observable test functions serving as basis functions, we verify if \mathcal{T}_τ is representable as a finite-rank operator.

We first look at the following property of \mathcal{T}_τ .

Proposition 4.4: For any $\lambda > \omega$, the operator \mathcal{T}_τ is compact if and only if \mathcal{K}_s is compact for any $s \in (0, \tau]$.

Proof: We assume that \mathcal{T}_τ is compact for $\lambda > \omega$. By [25, Theorem 3.2], \mathcal{K}_s is continuous w.r.t. the uniform operator norm $\|\cdot\|$. We can also easily verify the compactness of $\lambda \mathcal{T}_\tau \mathcal{K}_s$, for any $s \in (0, \tau]$, by Definition 4.1. In addition, for any arbitrarily small $t > 0$,

$$\begin{aligned} & \|\lambda \mathcal{T}_\tau \mathcal{K}_s - \mathcal{K}_s\| \\ & \leq \int_0^t \lambda e^{-\lambda \sigma} \|\mathcal{K}_{s+\sigma} - \mathcal{K}_s\| d\sigma + \int_t^\tau \lambda e^{-\lambda \sigma} \|\mathcal{K}_{s+\sigma} - \mathcal{K}_s\| d\sigma \\ & \leq \sup_{\sigma \in (0, t]} \|\mathcal{K}_{s+\sigma} - \mathcal{K}_s\| (1 - e^{-\lambda t}) + 2 \int_t^\tau \lambda e^{-\lambda \sigma} \|\mathcal{K}_\tau\| d\sigma \\ & \leq \sup_{\sigma \in (0, t]} \|\mathcal{K}_{s+\sigma} - \mathcal{K}_s\| + \frac{2M\lambda}{\lambda - \omega} e^{\omega(t+\tau) - \lambda t}. \end{aligned}$$

By the continuity of \mathcal{K}_s , letting $\lambda \rightarrow \infty$ and $t \rightarrow 0$, we have $\mathcal{K}_s \rightarrow \lambda \mathcal{T}_\tau \mathcal{K}_s$ in the uniform sense, which shows the compactness.

To show the converse side, we notice that the operator $\mathcal{T}_\tau^t := \int_t^\tau e^{-\lambda s} \mathcal{K}_s ds$ is always compact for any $t \in (0, \tau]$ given the compactness of \mathcal{K}_s with $s \in (0, \tau]$. However,

$$\begin{aligned} \|\mathcal{T}_\tau - \mathcal{T}_\tau^t\| & \leq \int_0^t e^{-\lambda s} \|\mathcal{K}_s\| ds \leq \int_0^t \|\mathcal{K}_s\| ds \\ & \leq \int_0^t M e^{\omega s} ds \leq t M e^{\omega t}. \end{aligned}$$

Letting $t \rightarrow 0$, we see the uniform convergence of \mathcal{T}_τ^t to \mathcal{T}_τ , which shows compactness of \mathcal{T}_τ . \blacksquare

It is worth noting that \mathcal{K}_t of (1) is not necessarily compact for each $t > 0$. To show that $\mathcal{K}_t(\mathcal{B}_r) \subseteq C(\mathcal{X})$ is relatively compact, where $\mathcal{B}_r = \{h \in C(\mathcal{R}) : |h|_\infty \leq r\}$ for some $r > 0$, one needs to verify the equicontinuity within $\mathcal{K}_t(\mathcal{B}_r)$. However, this is not guaranteed. As a counterexample, we

set $\mathcal{X} := (-1, 1)$, $h_n(x) = \sin(nx) \in \mathcal{B}_1$ (or similarly, for the Fourier basis), and define $\phi(t, x) = x \cdot e^{-t}$ for all $x \in \mathcal{X}$. Then, the sequence $h_n \circ \phi(t, \cdot)$ for each t does not exhibit equicontinuity due to the rapid oscillation as n increases.

For the purpose of approximating \mathcal{L} strongly, we aim to find a compact approximation of $\{\mathcal{K}_s\}_{s>0}$ that enables a finite-rank representation of \mathcal{T}_τ in the same sense.

Proposition 4.5: For each $t > 0$, there exists a family of compact linear operator $\{\mathcal{K}_t^\varepsilon\}_{\varepsilon>0}$, such that $\mathcal{K}_t^\varepsilon \rightarrow \mathcal{K}_t$ on $C(\mathcal{X})$ as $\varepsilon \rightarrow 0$. In addition, for each $t, s > 0$, there exists a family of compact linear operator $\{\mathcal{K}_i^\varepsilon\}_{\varepsilon>0}$, such that $\mathcal{K}_t^\varepsilon \circ \mathcal{K}_s^\varepsilon \rightarrow \mathcal{K}_t \circ \mathcal{K}_s$ on $h \in C(\mathcal{X})$ as $\varepsilon \rightarrow 0$.

We omit the proof, as it follows similar arguments presented in [7, Section V.A]. Heuristically, the semigroup $\{\mathcal{K}_t\}_{t>0}$ characterizes the flow of point masses of the system (1), where each point mass is considered to be distributed by a Dirac measure centered at its respective point in the flow. The compact approximation is achieved through the introduction of smooth mollifiers. Taking advantage of the compactness approximation, the following statement demonstrates the feasibility of approximating \mathcal{T}_τ by a finite-dimensional operator.

Corollary 4.6: For any fixed $\tau > 0$, for any arbitrarily small $\vartheta > 0$, there exists a sufficiently large N and a finite-dimensional approximation \mathcal{T}_τ^N such that $|\mathcal{T}_\tau^N h - \mathcal{T}_\tau h|_\infty < \vartheta$, $h \in C(\mathcal{X})$.

The proof is completed in Appendix I.

Remark 4.7: Similar to [7, Section V.B], one can consider a Hilbert space $\mathcal{H} := L^2(\mathcal{X}) \supseteq C(\mathcal{X})$ as a special case. Let $\{\varphi_i\}_{i \in \mathbb{Z}} \subseteq \mathcal{H}$ be the possibly complex-valued eigenfunctions of $\mathcal{K}_t^\varepsilon$. Then, $\mathcal{K}_t^\varepsilon \cdot = \sum_{i \in \mathbb{Z}} \rho_i^\varepsilon \langle \cdot, \bar{\varphi}_i \rangle \varphi_i$ can be approximated by a finite-sum $\mathcal{K}_t^N \cdot = \sum_{i=-N}^N \rho_i^\varepsilon \langle \cdot, \bar{\varphi}_i \rangle \varphi_i$, where $\{\rho_i^\varepsilon\}_{i \in \mathbb{Z}}$ represents the set of eigenvalues of $\{\mathcal{K}_t^\varepsilon\}_{t \geq 0}$ and $\langle \bar{\varphi}_i, \varphi_i \rangle = 1$ for all i . Then, \mathcal{T}_τ^N can be defined accordingly as shown in the proof of Corollary 4.6. \diamond

When dealing with linear operators in finite-dimensional spaces, the concept of basis equivalence ensures that different representations corresponding to different bases are related through similarity transformations. Thus, the operator's inherent properties remain invariant under a change of basis. Building on the feasibility of finite-dimensional approximation, the next section will investigate how to train \mathcal{L}_λ using a finite dictionary of test functions.

V. DATA-DRIVEN ALGORITHM

Recall Definition 4.1 and (18). Similar to the approximation of Koopman operators [7], [17], [27], obtaining a fully discretized version \mathbf{L} of the bounded linear operator $\lambda^2 \mathcal{T}_\tau^N - \lambda \mathbf{I}$ based on the training data typically relies on the selection of a discrete dictionary of continuously differentiable observable test functions, denoted by

$$\mathcal{Z}_N(x) := [\mathfrak{z}_0(x), \mathfrak{z}_1(x), \dots, \mathfrak{z}_{N-1}(x)], \quad N \in \mathbb{N}. \quad (19)$$

Then, the followings should hold:

1) Let $(\mu_i, \xi_i)_{i=0}^{N-1}$ be the eigenvalues and eigenvectors of \mathbf{L} . Let $(\rho_i, \varphi_i)_{i=0}^{N-1}$ be the eigenvalues and eigenfunctions of

\mathcal{L} . Then, for each i ,

$$\mu_i \approx \rho_i, \quad \varphi_i(x) \approx \mathcal{Z}_N(x)\xi_i. \quad (20)$$

2) For any $h \in \text{span}\{\mathfrak{z}_0, \mathfrak{z}_1, \dots, \mathfrak{z}_{N-1}\}$ such that $h(x) = \mathcal{Z}_N(x)\mathbf{w}$ for some column vector \mathbf{w} , we have that

$$\mathcal{L}h(\cdot) \approx \tilde{\mathcal{L}}_\lambda h(\cdot) \approx \lambda^2 \mathcal{T}_\tau^N h(\cdot) - \lambda h(\cdot) \approx \mathcal{Z}_N(\cdot)(\mathbf{L}\mathbf{w}). \quad (21)$$

In this section, we modify the existing Koopman learning technique to obtain \mathbf{L} .

A. Generating Training Data

For any fixed $\lambda > 0$, given a dictionary \mathcal{Z}_N of the form (19), for each $\mathfrak{z}_i \in \mathcal{Z}_N$ and each $x \in \mathcal{X}$, we consider $\mathfrak{z}_i(x)$ as the features and $\lambda^2 \mathcal{T}_\tau \mathfrak{z}_i(x) - \lambda \mathfrak{z}_i(x) = \lambda^2 \int_0^\tau e^{-\lambda s} \mathfrak{z}_i(\phi(s, x)) ds - \lambda \mathfrak{z}_i(x)$ as the labels. To compute the integral, we employ numerical quadrature techniques for approximation. This approach inevitably requires discrete-time observations (snapshots), the number of which is denoted by N , within the interval $[0, \tau]$ of the flow map $\phi(\tau, x)$.

To streamline the evaluation process for numerical examples, drawing inspiration from [28], for any τ and i , we can assess both the trajectory and the integral, i.e. the pair $(\phi(\tau, x), \lambda^2 \int_0^\tau e^{-\lambda s} \mathfrak{z}_i(\phi(s, x)) ds)$, by numerically solving the following augmented ODE system

$$\begin{aligned} \dot{\mathbf{x}}(t) &= f(\mathbf{x}(t)), \quad \mathbf{x}(0) = x \in \mathbb{R}^n, \\ \dot{I}_i(t) &= \lambda^2 e^{-\lambda t} \mathfrak{z}_i(\mathbf{x}), \quad I_i(0) = 0. \end{aligned} \quad (22)$$

We summarize the algorithm for generating training data for one time period as in Algorithm 1.

Algorithm 1 Generating Training Data

Require: f , n , N , \mathcal{X} , \mathcal{Z}_N , τ , λ , and uniformly sampled $\{x^{(m)}\}_{m=0}^{M-1} \subseteq \mathcal{X}$.

for m **from** 0 **to** $M - 1$ **do**
 for i **from** 0 **to** $N - 1$ **do**
 Compute $\mathfrak{z}_i(x^{(m)})$
 Compute $\lambda^2 \mathcal{T}_\tau \mathfrak{z}_i(x^{(m)})$ using (22)
 end for
 Stack

$$\tilde{\mathcal{L}}_\lambda \mathcal{Z}_N(x^{(m)}) = [\lambda^2 \mathcal{T}_\tau \mathfrak{z}_0(x^{(m)}) - \lambda \mathfrak{z}_0(x^{(m)}), \dots, \lambda^2 \mathcal{T}_\tau \mathfrak{z}_{N-1}(x^{(m)}) - \lambda \mathfrak{z}_{N-1}(x^{(m)})]$$

end for

Stack $\mathfrak{X}, \mathfrak{Y} \in \mathbb{C}^{M \times N}$ such that $\mathfrak{X} = [\mathcal{Z}_N(x^{(0)}), \mathcal{Z}_N(x^{(1)}), \dots, \mathcal{Z}_N(x^{(M-1)})]^T$ and $\mathfrak{Y} = [\tilde{\mathcal{L}}_\lambda \mathcal{Z}_N(x^{(0)}), \tilde{\mathcal{L}}_\lambda \mathcal{Z}_N(x^{(1)}), \dots, \tilde{\mathcal{L}}_\lambda \mathcal{Z}_N(x^{(M-1)})]^T$

B. Extended Dynamic Mode Decomposition Algorithm

After obtaining the training data $(\mathfrak{X}, \mathfrak{Y})$ using Algorithm 1, we can find \mathbf{L} by $\mathbf{L} = \text{argmin}_{A \in \mathbb{C}^{N \times N}} \|\mathfrak{Y} - \mathfrak{X}A\|_F$. The \mathbf{L} is given in closed-form as $\mathbf{L} = (\mathfrak{X}^T \mathfrak{X})^\dagger \mathfrak{X}^T \mathfrak{Y}$, where \dagger is the pseudo inverse. Similar to Extended Dynamic Mode Decomposition (EDMD) [27] for learning Koopman operators, the approximations (20) and (21) can be guaranteed. In addition, by the universal approximation theorem, all of

the function approximations from above should have uniform convergence to the actual quantities.

It is worth noting that operator learning frameworks, such as autoencoders, which utilize neural networks (NN) as dictionary functions, can reduce human bias in the selection of these functions [5]. Incorporating the proposed learning scheme with NN falls outside the scope of this paper but will be pursued in future work.

Remark 5.1 (The Logarithm Method): We compare the aforementioned learning approach of \mathcal{L} to those obtained using the benchmark approach as described in [17]. Briefly speaking, at a given $s \in [0, \tau]$, that method first obtains a matrix $\mathbf{K} \in \mathbb{C}^{N \times N}$ such that $\mathbf{K} = (\mathfrak{X}^T \mathfrak{X})^\dagger \mathfrak{X}^T \mathfrak{Y}$, where $\mathfrak{Y} = [\mathcal{Z}_N(\phi(s, x^{(0)}), \mathcal{Z}_N(\phi(s, x^{(1)}), \dots, \mathcal{Z}_N(\phi(s, x^{(M-1)}))]^T$. Let $(\mu_i^K, \xi_i^K)_{i=0}^{N-1}$ be the eigenvalues and eigenvectors of \mathbf{K} . Let $(\rho_i^K, \varphi_i^K)_{i=0}^{N-1}$ be the eigenvalues and eigenfunctions of \mathcal{K}_s . Similar to (20) and (21), for each i , we have $\varphi_i^K(x) \approx \mathcal{Z}_N(x)\xi_i^K$ and $\mathcal{K}_s h(\cdot) \approx \mathcal{Z}_N(\cdot)(\mathbf{K}\mathbf{w})$ for $h(x) = \mathcal{Z}_N(x)\mathbf{w}$.

However, even when \mathcal{L} can be represented by $(\log \mathcal{K}_s)/s$, we cannot guarantee that $\frac{\log \mathcal{K}_s}{s} h(\cdot) \approx \mathcal{Z}_N(\cdot)(\frac{\log(\mathbf{K})}{s}\mathbf{w})$, not to mention the case where the above logarithm representation does not hold. Denoting $\Phi(\cdot) = [\varphi_0^K(\cdot), \varphi_1^K(\cdot), \dots, \varphi_{N-1}^K(\cdot)]$ and $\Xi = [\xi_0^K, \xi_1^K, \dots, \xi_{N-1}^K]$, then it is clear that $\Phi(\cdot) = \mathcal{Z}_N(\cdot)\Xi$. In view of Remark 4.7, any $\mathcal{K}_s h(x)$ for any $h(x) = \mathcal{Z}_N(x)\mathbf{w}$ can be approximated using Φ . The (possibly complex-valued) rotation matrix Ξ establishes the connection between finite-dimensional eigenfunctions and dictionary functions through data-fitting, ensuring that any linear combination within \mathcal{Z}_N can be equivalently represented using Φ with a cancellation of the imaginary parts.

This imaginary-part cancellation effect does not generally hold when applying the matrix logarithm. Suppose the imaginary parts account for a significantly large value, the mutual representation of Φ and \mathcal{Z}_N does not match in the logarithmic scale. An exception holds unless the chosen dictionary is inherently rotation-free with respect to the true eigenfunctions [21], or there is direct access to the data for $\log(\mathcal{K}_s)$ allowing for direct training of the matrix. However, such conditions contravene our objective of leveraging Koopman data to conversely find the generator. In comparison, the approach in this paper presents an elegant method for approximating \mathcal{L} regardless of its boundedness. This enables the direct learning of \mathbf{L} without computing the logarithm, thereby avoiding the potential appearance of imaginary parts caused by basis rotation. \diamond

VI. CASE STUDY

We provide a numerical example to demonstrate the effectiveness of the proposed approach. The research code can be found at <https://github.com/Yiming-Meng/Log-Free-Learning-of-Koopman-Generators>.

Consider the Van der Pol oscillator

$$\dot{\mathbf{x}}_1(t) = \mathbf{x}_2(t), \quad \dot{\mathbf{x}}_2(t) = -\mathbf{x}_1(t) + (1 - \mathbf{x}_1^2(t))\mathbf{x}_2(t),$$

$\mathfrak{z}_{i,j}$	$j=0$	$j=1$	$j=2$
$i=0$	-1.6×10^{-10}	$\mathbf{1} + \mathbf{10}^{-6}$	-4.8×10^{-10}
$i=1$	-1.3×10^{-5}	-1.9×10^{-9}	-1.4×10^{-7}
$i=2$	-3.6×10^{-10}	-1.0×10^{-6}	-6.1×10^{-10}
$i=3$	-1.5×10^{-8}	-2.3×10^{-9}	-2.9×10^{-7}

TABLE I: The weights of \mathcal{Z}_N obtained by \mathbf{Le}_2 .

$\mathfrak{z}_{i,j}$	$j=0$	$j=1$	$j=2$
$i=0$	-3.8×10^{-10}	$\mathbf{1} - \mathbf{10}^{-5}$	1.3×10^{-9}
$i=1$	$-\mathbf{1} - \mathbf{10}^{-6}$	9.5×10^{-10}	-2.0×10^{-6}
$i=2$	8.1×10^{-10}	$-\mathbf{1} - \mathbf{10}^{-6}$	-2.0×10^{-9}
$i=3$	1×10^{-8}	-6.9×10^{-10}	-3.0×10^{-9}

TABLE II: The weights of \mathcal{Z}_N obtained by \mathbf{Le}_5 .

with $\mathbf{x}(0) = x := [x_1, x_2]$. We assume the system dynamics are unknown to us, and our information is limited to the system dimension, $n = 2$, and observations of sampled trajectories. To generate training data using Algorithm 1, for simplicity of illustration, we select $\mathcal{X} = (-1, 1)^2$ and obtain a total of $M = 100^2$ uniformly spaced samples $\{x^{(m)}\}_{m=0}^{M-1}$ in \mathcal{X} . We choose the dictionary as

$$\mathcal{Z}_N = [\mathfrak{z}_{0,0}, \mathfrak{z}_{1,0}, \dots, \mathfrak{z}_{3,0}, \mathfrak{z}_{0,1}, \mathfrak{z}_{1,1}, \mathfrak{z}_{2,1}, \dots, \mathfrak{z}_{i,j}, \dots, \mathfrak{z}_{3,2}], N = 12, \quad (23)$$

where $\mathfrak{z}_{i,j}(x_1, x_2) = x_1^i x_2^j$ for each $i \in \{0, 1, 2, 3\}$ and $j \in \{0, 1, 2\}$. We also set $\tau = 1$ and $\lambda = 10^6$. The discrete form \mathbf{L} can be obtained according to Section V-B. We apply the learned \mathbf{L} to identify the system vector fields, and construct a local Lyapunov function for the unknown system.

A. System Identification

The actual vector field is $f(x) := [f_1(x), f_2(x)] = [x_2, -x_1 + (1 - x_1^2)x_2]$. As we can analytically establish that $\mathcal{L}_{\lambda \mathfrak{z}_{1,0}}(x) = f_1(x)$ and $\mathcal{L}_{\lambda \mathfrak{z}_{0,1}}(x) = f_2(x)$, we use the approximation $[\mathcal{L}_{\lambda \mathfrak{z}_{1,0}}, \mathcal{L}_{\lambda \mathfrak{z}_{0,1}}]$ to conversely obtain f .

Note that $\mathfrak{z}_{1,0}(x) = \mathcal{Z}_N(x)\mathbf{e}_2$ and $\mathfrak{z}_{0,1}(x) = \mathcal{Z}_N(x)\mathbf{e}_5$, where each \mathbf{e}_i for $i \in \{0, 1, \dots, N\}$ is a column unit vector with all components being 0 except for the i -th component, which is 1. To apply \mathbf{L} , we have that $\mathcal{L}_{\lambda \mathfrak{z}_{1,0}}(x) \approx \mathcal{Z}_N(x)(\mathbf{Le}_2)$ and $\mathcal{L}_{\lambda \mathfrak{z}_{0,1}}(x) \approx \mathcal{Z}_N(x)(\mathbf{Le}_5)$.

In other words, we approximate $\mathcal{L}_{\lambda \mathfrak{z}_{1,0}}$ and $\mathcal{L}_{\lambda \mathfrak{z}_{0,1}}$ (and hence f_1 and f_2) using a linear combination of functions within \mathcal{Z}_N . The weights for these approximations are given by \mathbf{Le}_2 and \mathbf{Le}_5 , respectively. We report the corresponding results in Table I and II.

We compare the aforementioned results with those obtained using the benchmark approach as described in [17] with the same M and \mathcal{Z}_N . As described in Remark 5.1, $\mathbf{K} \in \mathbb{C}^{N \times N}$ can be obtained such that $\mathcal{K}_s \mathfrak{z}_{1,0}(x) \approx \mathcal{Z}_N(x)(\mathbf{Ke}_2)$ and $\mathcal{K}_s \mathfrak{z}_{0,1}(x) \approx \mathcal{Z}_N(x)(\mathbf{Ke}_5)$. Then, we have the approximation, as claimed by [17], $f_1(x) \approx \mathcal{Z}_N(x)(\log(\mathbf{K})\mathbf{e}_2/s)$ and $f_2(x) \approx \mathcal{Z}_N(x)(\log(\mathbf{K})\mathbf{e}_5/s)$ w.r.t. $|\cdot|_\infty$. According to [17, Section VI.A], we set $s = 0.5$ to avoid the multi-valued matrix logarithm. We report the weights obtained by taking the real parts of $\log(\mathbf{K})\mathbf{e}_2/s$ and $\log(\mathbf{K})\mathbf{e}_5/s$ in Table III and IV, respectively. Multiple orders of magnitude in accuracy have been established using the proposed method.

$\mathfrak{z}_{i,j}$	$j=0$	$j=1$	$j=2$
$i=0$	-9.5×10^{-16}	$\mathbf{1} - \mathbf{3.0} \times \mathbf{10}^{-4}$	-4.8×10^{-10}
$i=1$	$-\mathbf{4.1} \times \mathbf{10}^{-3}$	-3×10^{-15}	$-\mathbf{1.8} \times \mathbf{10}^{-2}$
$i=2$	-1.7×10^{-16}	$-\mathbf{6.4} \times \mathbf{10}^{-3}$	-7.8×10^{-17}
$i=3$	$-\mathbf{6.0} \times \mathbf{10}^{-3}$	-6.7×10^{-15}	$-\mathbf{3.7} \times \mathbf{10}^{-2}$

TABLE III: The weights of \mathcal{Z}_N obtained by $\log(\mathbf{K})\mathbf{e}_2/s$.

$\mathfrak{z}_{i,j}$	$j=0$	$j=1$	$j=2$
$i=0$	-8.6×10^{-16}	$\mathbf{1} + \mathbf{6.5} \times \mathbf{10}^{-3}$	4.1×10^{-16}
$i=1$	$-\mathbf{1} + \mathbf{3.0} \times \mathbf{10}^{-2}$	-1.6×10^{-15}	$-\mathbf{1.5} \times \mathbf{10}^{-1}$
$i=2$	1.0×10^{-15}	$-\mathbf{1} - \mathbf{3.8} \times \mathbf{10}^{-2}$	-2.0×10^{-15}
$i=3$	$-\mathbf{5.8} \times \mathbf{10}^{-2}$	1.8×10^{-15}	$\mathbf{3.3} \times \mathbf{10}^{-1}$

TABLE IV: The weights of \mathcal{Z}_N obtained by $\log(\mathbf{K})\mathbf{e}_5/s$.

It is worth noting that, unlike the experiment in [17] where $i, j \in \{0, 1, 2, 3\}$, we deliberately choose different numbers for i and j , leading to non-negligible imaginary parts after taking the matrix logarithm of \mathbf{K} . The imaginary parts of the learned weights using the Koopman-logarithm approach are reported in Appendix II. The presence of non-negligible imaginary parts indicates that the underlying system is sensitive to the selection of dictionary functions when employing the Koopman-logarithm approach, an effect that is significant and cannot be overlooked when aiming to minimize human intervention in identifying unknown systems in practice. Furthermore, the original experiment in [17] used $M = 300^2$ samples for a data fitting, and when M is reduced to 100^2 , the quality of the operator learning deteriorates.

B. Stability Prediction for the Reversed Dynamics

Observing the identified system dynamics, we anticipate that the time-reversed system is (locally) asymptotically stable w.r.t. the origin. We use the learned \mathbf{L} to construct polynomial Lyapunov functions based on the Lyapunov equation $\mathcal{L}V(x) = |x|^2$, where the sign on the r.h.s. is reversed due to the dynamics being reversed. To use \mathbf{L} and the library functions from \mathcal{Z}_N , we define the weights as $\theta := [\theta_0, \theta_1, \dots, \theta_{N-1}]^T$ and seek a θ such that $V(x; \theta) := \mathcal{Z}_N(x)\theta$, with the objective of minimizing $|\mathcal{Z}_N(x)\mathbf{L}\theta - x_1^2 - x_2^2|$. Ignoring the small terms of the magnitude 10^{-9} , the constructed Lyapunov function is given by $V(x; \theta) = 1.39x_1^2 - 1.56x_1x_2 + 1.16x_2^2 + 0.74x_1^2x_2^2$. Additionally, $\mathcal{L}V(x; \theta)$ is approximated by $\mathcal{Z}_N(x)\mathbf{L}\theta$, with the maximal value observed at $\mathcal{Z}_N(0)\mathbf{L}\theta = -0.068$, which indicates that stability prediction using the data-driven Lyapunov function is verified to be valid. This indicates that the stability prediction, as inferred using the data-driven Lyapunov function, is verified to be valid. The visualization can be found in Fig 1.

Remark 6.1: The idea illustrated above can be expanded to cover a larger region of interest. Specifically, a Zubov equation, instead of a Lyapunov equation, can be solved within the Koopman learning framework using the same dataset [7] as proposed in Algorithm 1. The solution obtained can potentially serve as a Lyapunov function. Since it cannot guarantee the properties of the learned function's derivatives,

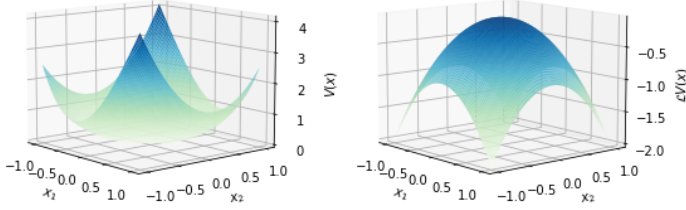


Fig. 1: Data-driven Lyapunov function V and its Lie derivative $\mathcal{L}V$ w.r.t. the predicted system dynamics.

to confirm it as a true Lyapunov function, the data can be reused as in Algorithm 1 to verify its Lie derivative. \diamond

VII. CONCLUSION

In this paper, we propose a logarithm-free Koopman operator-based learning framework for the infinitesimal generator, demonstrating both theoretical and numerical improvements over the method proposed in [17]. In particular, for more general cases where the generator is unbounded and, consequently, the logarithm of the Koopman operator cannot be used for representation, we draw upon the rich literature to propose an approximation (Eq. (18)) based on Yosida's approximation. A convergence result, along with the convergence rate, is proved in this paper to guide users in tuning the parameters. A numerical example with application in system identification is provided in comparison with the experiment in [17] demonstrating the learning accuracy. Unlike the experiment in [17], where learning accuracy is sensitive to the choice of dictionary functions, the method presented in this paper shows significant improvement in this regard. In applications where automatic computational approaches surpass human computability, such as in constructing Lyapunov-like functions using the Lie derivative, the proposed logarithm-free method holds more promise. We will pursue future efforts to provide more analysis on the sampling rate, numerical simulations, and real-world applications using real data.

REFERENCES

- [1] J. Sjöberg, Q. Zhang, L. Ljung, A. Benveniste, B. Delyon, P.-Y. Glorennec, H. Hjalmarsson, and A. Juditsky, "Nonlinear black-box modeling in system identification: a unified overview," *Automatica*, vol. 31, no. 12, pp. 1691–1724, 1995.
- [2] R. Haber and H. Unbehauen, "Structure identification of nonlinear dynamic systems—a survey on input/output approaches," *Automatica*, vol. 26, no. 4, pp. 651–677, 1990.
- [3] A. Mauroy and I. Mezić, "A spectral operator-theoretic framework for global stability," in *52nd IEEE Conference on Decision and Control*, pp. 5234–5239, IEEE, 2013.
- [4] A. Mauroy and I. Mezić, "Global stability analysis using the eigenfunctions of the Koopman operator," *IEEE Transactions on Automatic Control*, vol. 61, no. 11, pp. 3356–3369, 2016.
- [5] S. A. Deka, A. M. Valle, and C. J. Tomlin, "Koopman-based neural lyapunov functions for general attractors," in *61st Conference on Decision and Control (CDC)*, pp. 5123–5128, IEEE, 2022.
- [6] J. L. Proctor, S. L. Brunton, and J. N. Kutz, "Dynamic mode decomposition with control," *SIAM Journal on Applied Dynamical Systems*, vol. 15, no. 1, pp. 142–161, 2016.

- [7] Y. Meng, R. Zhou, and J. Liu, "Learning regions of attraction in unknown dynamical systems via Zubov-Koopman lifting: Regularities and convergence," *arXiv preprint arXiv:2311.15119*, 2023.
- [8] I. M. Mitchell, A. M. Bayen, and C. J. Tomlin, "A time-dependent Hamilton-Jacobi formulation of reachable sets for continuous dynamic games," *IEEE Transactions on Automatic Control*, vol. 50, no. 7, pp. 947–957, 2005.
- [9] Y. Lin, E. D. Sontag, and Y. Wang, "A smooth converse lyapunov theorem for robust stability," *SIAM Journal on Control and Optimization*, vol. 34, no. 1, pp. 124–160, 1996.
- [10] J. Liu, Y. Meng, M. Fitzsimmons, and R. Zhou, "Physics-informed neural network lyapunov functions: Pde characterization, learning, and verification," *arXiv preprint arXiv:2312.09131*, 2023.
- [11] Y. Meng, Y. Li, M. Fitzsimmons, and J. Liu, "Smooth converse Lyapunov-barrier theorems for asymptotic stability with safety constraints and reach-avoid-stay specifications," *Automatica*, vol. 144, p. 110478, 2022.
- [12] Y. Meng and J. Liu, "Lyapunov-barrier characterization of robust reach-avoid-stay specifications for hybrid systems," *Nonlinear Analysis: Hybrid Systems*, vol. 49, p. 101340, 2023.
- [13] W. Pan, Y. Yuan, J. Gonçalves, and G.-B. Stan, "A sparse bayesian approach to the identification of nonlinear state-space systems," *IEEE Transactions on Automatic Control*, vol. 61, no. 1, pp. 182–187, 2015.
- [14] S. L. Brunton, J. L. Proctor, and J. N. Kutz, "Discovering governing equations from data by sparse identification of nonlinear dynamical systems," *Proceedings of the National Academy of Sciences*, vol. 113, no. 15, pp. 3932–3937, 2016.
- [15] J. C. Nash and M. Walker-Smith, "Nonlinear parameter estimation," *An integrated system on BASIC. NY, Basel*, vol. 493, 1987.
- [16] J. M. Varah, "A spline least squares method for numerical parameter estimation in differential equations," *SIAM Journal on Scientific and Statistical Computing*, vol. 3, no. 1, pp. 28–46, 1982.
- [17] A. Mauroy and J. Gonçalves, "Koopman-based lifting techniques for nonlinear systems identification," *IEEE Transactions on Automatic Control*, vol. 65, no. 6, pp. 2550–2565, 2019.
- [18] S. Klus, F. Nüske, S. Peitz, J.-H. Niemann, C. Clementi, and C. Schütte, "Data-driven approximation of the Koopman generator: Model reduction, system identification, and control," *Physica D: Nonlinear Phenomena*, vol. 406, p. 132416, 2020.
- [19] Z. Drmač, I. Mezić, and R. Mohr, "Identification of nonlinear systems using the infinitesimal generator of the Koopman semigroup—a numerical implementation of the Mauroy–Goncalves method," *Mathematics*, vol. 9, no. 17, p. 2075, 2021.
- [20] M. Black and D. Panagou, "Safe control design for unknown nonlinear systems with koopman-based fixed-time identification," *IFAC-PapersOnLine*, vol. 56, no. 2, pp. 11369–11376, 2023.
- [21] Z. Zeng, Z. Yue, A. Mauroy, J. Gonçalves, and Y. Yuan, "A sampling theorem for exact identification of continuous-time nonlinear dynamical systems," in *2022 IEEE 61st Conference on Decision and Control (CDC)*, pp. 6686–6692, IEEE, 2022.
- [22] Z. Zeng and Y. Yuan, "A generalized nyquist-shannon sampling theorem using the koopman operator," *arXiv preprint*, 2023.
- [23] A. Nejati, A. Lavaei, S. Soudjani, and M. Zamani, "Data-driven estimation of infinitesimal generators of stochastic systems," *IFAC-PapersOnLine*, vol. 54, no. 5, pp. 277–282, 2021.
- [24] C. Wang, Y. Meng, S. L. Smith, and J. Liu, "Data-driven learning of safety-critical control with stochastic control barrier functions," in *61st Conference on Decision and Control (CDC)*, pp. 5309–5315, IEEE, 2022.
- [25] A. Pazy, *Semigroups of Linear Operators and Applications to Partial Differential Equations*, vol. 44. Springer Science & Business Media, 2012.
- [26] J. C. Willems, "Dissipative dynamical systems part i: General theory," *Archive for Rational Mechanics and Analysis*, vol. 45, no. 5, pp. 321–351, 1972.
- [27] M. O. Williams, I. G. Kevrekidis, and C. W. Rowley, "A data-driven approximation of the Koopman operator: Extending dynamic mode decomposition," *Journal of Nonlinear Science*, vol. 25, pp. 1307–1346, 2015.
- [28] W. Kang, K. Sun, and L. Xu, "Data-driven computational methods for the domain of attraction and Zubov's equation," *IEEE Transactions on Automatic Control*, 2023.

APPENDIX I
PROOFS IN TECHNICAL RESULTS

Proof of Proposition 3.5: For all $h \in C^1(\mathcal{X})$ and $x \in \mathcal{X}$, we have

$$\begin{aligned}
& R(\lambda)(\lambda I - \mathcal{L})h(x) \\
&= \lambda R(\lambda)h(x) - R(\lambda)\mathcal{L}h(x) \\
&= \lambda \int_0^\infty e^{-\lambda t} h(\phi(t, x)) dt - \int_0^\infty e^{-\lambda t} \mathcal{L}h(\phi(t, x)) dt \\
&= -h(\phi(t, x))e^{-\lambda t} \Big|_0^\infty + \int_0^\infty e^{-\lambda t} d(h(\phi(t, x))) \\
&\quad - \int_0^\infty e^{-\lambda t} \mathcal{L}h(\phi(t, x)) dt \\
&= h(\phi(0, x)) = h(x),
\end{aligned} \tag{24}$$

where we have used the fact that the time derivative along the trajectories of (1) is such that $dh(x)/dt = \mathcal{L}h(x)$.

On the other hand, for all $h \in C(\mathcal{X})$, all $x \in \mathcal{X}$, and all $t \geq 0$,

$$\begin{aligned}
& R(\lambda)h(x) \\
&= \int_0^t \mathcal{K}_{s, -\lambda} h(x) ds + \int_t^\infty \mathcal{K}_{s, -\lambda} h(x) ds \\
&= \int_0^t \mathcal{K}_{s, -\lambda} h(x) ds + \int_0^\infty \mathcal{K}_{t+s, -\lambda} h(x) ds \\
&= \int_0^t \mathcal{K}_{s, -\lambda} h(x) ds + \int_0^\infty e^{-(t+s)\lambda} \mathcal{K}_s h(\phi(t, x)) ds \\
&= \int_0^t e^{-\lambda s} \mathcal{K}_s h(x) ds + e^{-\lambda t} R(\lambda)h(\phi(t, x)).
\end{aligned} \tag{25}$$

However,

$$\mathcal{K}_t R(\lambda)h(x) = \int_0^\infty e^{-\lambda s} \mathcal{K}_s h(\phi(t, x)) ds = R(\lambda)\mathcal{K}_t h(x). \tag{26}$$

Therefore,

$$\begin{aligned}
& \frac{\mathcal{K}_t R(\lambda)h(x) - R(\lambda)h(x)}{t} \\
&= \frac{\mathcal{K}_t R(\lambda)h(x) - e^{-\lambda t} R(\lambda)h(\phi(t, x))}{t} \\
&\quad + \frac{e^{-\lambda t} R(\lambda)h(\phi(t, x)) - R(\lambda)h(x)}{t} \\
&= \frac{\mathcal{K}_t R(\lambda)h(x) - e^{-\lambda t} \mathcal{K}_t R(\lambda)h(x)}{t} - \frac{1}{t} \int_0^t e^{-\lambda s} \mathcal{K}_s h(x) ds.
\end{aligned} \tag{27}$$

Sending $t \rightarrow 0$ on both sides, we have

$$\mathcal{L}R(\lambda)h(x) = \lambda R(\lambda)h(x) - h(x), \tag{28}$$

which is equivalent as $(\lambda I - \mathcal{L})R(\lambda)h(x) = h(x)$. ■

Proof of Corollary 4.6: We show the sketch of the proof. Working on the compact family of $\{\mathcal{K}_s^\varepsilon\}_{s \in (0, \tau]}$ for some small $\varepsilon > 0$, one can find a sufficiently large N such that

$$|\mathcal{K}_s^N h - \mathcal{K}_s h|_\infty < \vartheta, \quad h \in C(\mathcal{X}), \quad s \in (0, \tau],$$

$\delta_{i,j}$	$j=0$	$j=1$	$j=2$
$i=0$	-1.8×10^{-17}	2.0×10^{-3}	-2.2×10^{-18}
$i=1$	5.3×10^{-3}	6.9×10^{-17}	-2.3×10^{-2}
$i=2$	1.6×10^{-17}	-8.4×10^{-3}	-3.0×10^{-17}
$i=3$	-8.4×10^{-3}	-1.1×10^{-16}	5.0×10^{-2}

TABLE V: The imaginary parts obtained by $\log(\mathbf{K})\mathbf{e}_2/s$.

$\delta_{i,j}$	$j=0$	$j=1$	$j=2$
$i=0$	-8.0×10^{-17}	8.8×10^{-3}	-9.5×10^{-18}
$i=1$	2.3×10^{-2}	3.0×10^{-16}	-1.0×10^{-1}
$i=2$	6.9×10^{-17}	-3.7×10^{-2}	-1.3×10^{-16}
$i=3$	3.7×10^{-2}	-4.9×10^{-16}	2.2×10^{-1}

TABLE VI: The imaginary parts obtained by obtained by $\log(\mathbf{K})\mathbf{e}_5/s$.

where K_s^N is the finite-dimensional representation of K_s^ε . Let $\mathcal{T}_\tau^N := \int_0^\tau e^{-\lambda s} \mathcal{K}_s^N ds$. Then, for any $t \in (0, \tau)$,

$$\begin{aligned}
& |\mathcal{T}_\tau^N h - \mathcal{T}_\tau h|_\infty \\
&\leq \int_0^t e^{-\lambda s} |\mathcal{K}_s^N h - \mathcal{K}_s h|_\infty ds + \int_t^\tau e^{-\lambda s} |\mathcal{K}_s^N h - \mathcal{K}_s h|_\infty ds \\
&\leq C|h|_\infty t + \sup_{s \in (0, \tau]} |\mathcal{K}_s^N h - \mathcal{K}_s h|_\infty \cdot \frac{e^{-\lambda t} - e^{-\lambda \tau}}{\lambda} \\
&< C|h|_\infty t + \vartheta,
\end{aligned} \tag{29}$$

where $C := \sup_{s \in (0, t]} \|K_s^N\| + M e^{\omega t}$. The conclusion follows by sending $t \rightarrow 0$. ■

APPENDIX II
SUPPLEMENTARY RESULTS IN SECTION VI

We present the imaginary parts of $\log(\mathbf{K})\mathbf{e}_2/s$ and $\log(\mathbf{K})\mathbf{e}_5/s$ in this section. The results are reported in Table V and Table VI, respectively.